

tion that all broadening in  $\alpha$ -Si is due to surface chemical shifts of atoms surrounding voids. It must rather be attributed to random charge fluctuations as the result of bond length variations in the amorphous network. The average rms charge deviation is estimated to be 0.11 electron in  $\alpha$ -Si, only about half as much as obtained by Guttman, Ching, and Rath. In  $\alpha$ -Si:H the incorporation of hydrogen leads apparently to an overall reduction in the bond length fluctuations as manifested in the reduced  $\sigma_{\text{amorph}}$ , corresponding to charge fluctuations of only 0.09 electron. This is in agreement with the 20% attenuation of the TO bands in the ir spectrum of  $\alpha$ -Si upon hydrogenation.<sup>5</sup>

We thank the staff of HasyLab for their kind hospitality and in particular C. Kunz for making his spectrometer available to us.

<sup>1</sup>See, e.g., N. F. Mott and E. A. Davis, *Electronic Processes in Non-crystalline Materials* (Clarendon, Oxford, 1979).

<sup>2</sup>P. W. Anderson, B. I. Halperin, and C. M. Varma,

*Philos. Mag.* **25**, 1 (1972).

<sup>3</sup>L. Guttman, W. Y. Ching, and J. Rath, *Phys. Rev. Lett.* **44**, 1513 (1980).

<sup>4</sup>See, e.g., M. Brodsky and A. Lurio, *Phys. Rev. B* **9**, 1646 (1974).

<sup>5</sup>S. C. Shen, C. J. Fang, M. Cardona, and L. Genzel, *Phys. Rev. B* **22**, 2913 (1980).

<sup>6</sup>F. J. Grunthaner, P. J. Grunthaner, R. P. Vasquez, B. F. Lewis, J. Maserjian, and A. Madhukar, *Phys. Rev. Lett.* **43**, 1683 (1979).

<sup>7</sup>S. C. Moss and J. F. Graczyk, *Phys. Rev. Lett.* **21**, 1575 (1969).

<sup>8</sup>There is as yet no general agreement on the exact magnitude of the surface shift on Si(111). See, e.g., S. Brennan, J. Stöhr, R. Jaeger, and J. E. Rowe, *Phys. Rev. Lett.* **45**, 1414 (1980), and F. J. Himpsel, P. Heimann, T. C. Chiang, and D. E. Eastman, *Phys. Rev. Lett.* **45**, 1112 (1980).

<sup>9</sup>K. J. Gruntz, L. Ley, and R. L. Johnson, *Phys. Rev. B* **24**, 2069 (1981).

<sup>10</sup>P. Kelfve, B. Blomster, H. Siegbahn, K. Siegbahn, E. Sanhueza, and O. Goscinski, *Phys. Scr.* **21**, 75 (1980).

<sup>11</sup>B. Kramer, H. King, and A. McKinnon, in *Proceedings of the Sixteenth International Conference on the Physics of Semiconductors*, Montpellier, 1982 (to be published). We thank the authors for private communication of their results.

## Thermal Excitation of Two-Dimensional Plasma Oscillations

Ralph A. Höpfel, Erich Vass, and Erich Gornik

*Institut für Experimentalphysik, Universität Innsbruck, A-6020 Innsbruck, Austria*

(Received 16 August 1982)

Experimental evidence for thermal excitation of plasmons in two-dimensional electron systems is reported. The spectral intensity and temperature dependence of the thermal excitation are calculated by means of Bose-Einstein statistics, and give quantitative agreement with the results of far-infrared emission experiments. It is found that the plasmons may contribute significantly to the specific heat of the two-dimensional electron system at low electron densities and high temperatures.

PACS numbers: 73.40.Qv, 65.40.-f, 71.45.Gm, 72.30.+q

Longitudinal plasma waves in two-dimensional electron systems (2D plasmons) exhibit a different dispersion behavior from 3D carrier systems and have therefore been the subject of intense experimental and theoretical investigations.<sup>1-5</sup> The dispersion relation  $\omega(k)$  has been verified with high accuracy by far-infrared (FIR) absorption<sup>6</sup> and emission,<sup>7</sup> and recently by light-scattering<sup>8</sup> experiments. For strictly two-dimensional plasmons one obtains a dispersion relation<sup>5</sup>  $\omega$  proportional to  $k^{1/2}$ ; for coupled plasmon modes of lay-

ered 2D electron systems the frequency is approximately a linear function<sup>8</sup> of the wave vector  $k$ . In the present work it will be shown that plasmons in 2D and layered electron systems can be excited thermally by heating the electron gas with an external electric field. The spectral intensity of the excitation will depend on the temperature and density of the plasma.

The spectral intensity of the longitudinal two-dimensional plasmons is calculated with Bose-Einstein statistics.<sup>9</sup> The criterion for well-de-

finned plasma excitations,<sup>10</sup>  $\omega\tau_{\text{pl}} \gg 1$ , where  $\tau_{\text{pl}}$  is the lifetime of the plasma excitation, is fulfilled reasonably well in our experiments with a value of  $\omega\tau_{\text{pl}}$  approximately equal to 10. For an arbitrary plasmon dispersion relation  $\omega(k)$ , the plasmon energy density is given by

$$U(\omega(k), T) = \int u(\omega(k), T) d\omega,$$

where the spectral energy density  $u(\omega(k), T)$  is

$$u(\omega(k), T) = \frac{1}{(2\pi)^2} \int \frac{\hbar\omega(k)k(\delta k/\delta\omega)d\varphi}{\exp[\hbar\omega(k)/k_B T] - 1}. \quad (1)$$

$\varphi$  is the polar angle in the two-dimensional  $k$  space and  $(\delta k/\delta\omega)$  is the inverse of the group velocity of the plasmon  $\omega(k)$ .  $T$  denotes the electron temperature.

In order for radiation from 2D plasmons, which are nonradiative excitations,<sup>1</sup> to be observed, they have to be coupled to the electromagnetic field. This is achieved by a metallic grating that allows the radiative decay of modes with the wave vector defined by the grating.<sup>6,7</sup> The emitted power per unit area for a given wave vector  $k$  in the interval  $(\omega, \omega + d\omega)$  can be written as

$$\frac{\delta u(\omega(k), T)}{\delta t} d\omega = \frac{1}{(2\pi)^2} \frac{\hbar\omega k \pi (\delta k/\delta\omega)}{\exp(\hbar\omega/k_B T) - 1} \frac{1}{\tau_{\text{rad}}} d\omega. \quad (2)$$

The factor  $\pi$  in the numerator is due to the line structure of the grating that couples only about half of the excited plasmons to the radiation field.  $\tau_{\text{rad}}$  is the radiative decay time of the plasmon via the grating antenna, given by  $\tau_{\text{rad}} = (2\pi/\omega)/\alpha$ , where  $\alpha$  denotes the efficiency of the grating with  $0 \leq \alpha \leq 1$ . In our experiments the electrons are

$$\frac{\delta u(\omega(k), T)}{\delta t} = \frac{1}{(2\pi)^2} \frac{\hbar\omega k^2 \alpha}{1 + \omega^2 m^* \epsilon_0 \epsilon_i d / n_s e^2 \sinh^2(kd)} \frac{1}{\exp(\hbar\omega/k_B T) - 1}. \quad (4)$$

The calculated spectral intensity  $\delta u(\omega(k), T)/\delta t$  is shown in Fig. 1 as a function of  $k$  at different electron temperatures for a fixed electron density  $n_s$  in a Si MOS structure. Equation (4) is the analog to the Planck radiation law for 2D plasma oscillations. The equation describes the theoretical dependence of the thermal excitation spectrum on frequency, electron temperature, wave vector, and electron density: The excitation increases exponentially with the electron temperature, and for a given frequency the excitation increases with about  $k^2$ , which is—if we neglect screening by the gate—proportional to  $n_s^{-2}$ . This means that the amount of plasmon excitation should increase with decreasing density of the

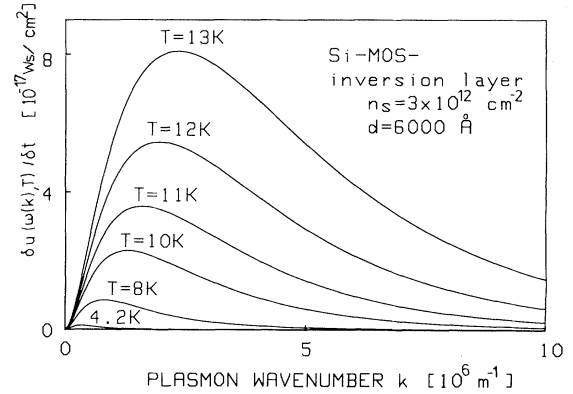


FIG. 1. Spectral radiation power density  $\delta u(\omega(k), T)/\delta t$  as a function of the plasmon wave number for a 2D electron plasma of constant density at different electron temperatures. The antenna efficiency is  $\alpha = 1$ .

heated by an electric field; therefore for Eq. (2) to be valid it is necessary that the electron-plasmon scattering is strong enough to guarantee a plasmon distribution according to Eq. (1) and is not influenced by the emission. This requires  $\tau_{\text{rad}} \gg \tau_{\text{pl}}$ . The dispersion relation of longitudinal 2D plasmons in, e.g., Si MOSFETs (metal-oxide-semiconductor field-effect transistors), screened by a metallic gate, is given by<sup>2</sup>

$$\omega^2 = \frac{n_s e^2}{m^* \epsilon_0} \frac{k}{\epsilon_s + \epsilon_i \coth(kd)}, \quad (3)$$

where  $n_s$  is the carrier density,  $d$  the oxide thickness, and  $\epsilon_s$  and  $\epsilon_i$  the dielectric constants of the surrounding media. The spectral intensity of the radiation from thermally excited plasmons is obtained from Eqs. (2) and (3) as

plasma. For the radiation intensity the  $k$  dependence of  $\alpha$ —given below in Eq. (5)—must be considered.

We give the experimental evidence for thermal excitation of two-dimensional plasmons and their spectral emission by investigating the FIR narrow-band emission that results from the radiative decay of 2D plasmons as described in Ref. 7: The samples are (100) Si MOSFETs with peak mobilities of 18 000 cm<sup>2</sup>/V s and oxide thicknesses from 1400 to 6000 Å. Upon the semitransparent Ti-gate electrodes, Al gratings of periods 3, 2, and 1.5 μm were evaporated. The electron temperature was increased over 4.2 K by application

of pulsed electric source-drain fields of 1 to 100 V/cm. The emission is detected by high-purity GaAs detectors at 4.4 meV with a resolution of  $2.0 \text{ cm}^{-1}$  and a sensitivity of  $10^6 \text{ V/W}$ .

The performed emission experiments allow us to test the theory of thermal excitation outlined above, and allow us to verify *quantitatively* the radiation formula, since all parameters  $T$ ,  $\omega$ ,  $k$ , and  $n_s$  can be varied and are known. The factor for the antenna efficiency is given by<sup>6</sup>

$$\alpha = \frac{\beta [\coth^2(kd) - 1]}{[\epsilon_s/\epsilon_i + \coth(kd)]^2}, \quad (5)$$

where the geometry factor  $\beta$  takes into account the grating design.<sup>6</sup> Our emission experiments show that the absolute values of the total plasmon emission intensity, which are on the order of  $10^{-7}$  to  $10^{-6} \text{ W/cm}^2$ , agree accurately with the radiation power calculated from Eq. (4) without use of any fitting parameters. The dependence of the radiated power on the electric field and thus on the electron temperature is exactly described by Eq. (4) up to  $T = 13 \text{ K}$  as demonstrated in Fig. 2: The calculated intensity is compared with the experimental data divided by the antenna efficiency. This quantity is a direct measure for the amount of the thermal plasmon excitation. The electron temperatures as a function of the electric field were determined from the amplitudes of Shubnikov-de Haas oscillations and by evaluating

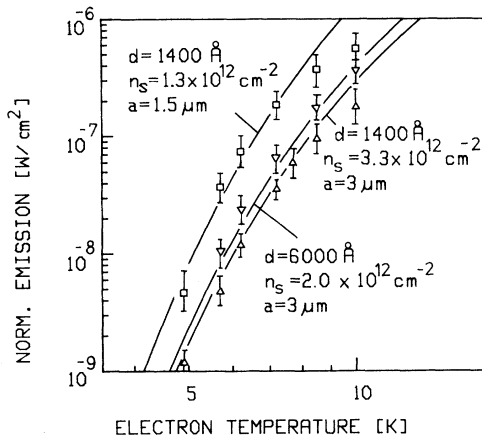


FIG. 2. Theoretical [Eq. (4)] and experimental plasmon excitation at  $\hbar\omega = 4.4 \text{ meV}$  as a function of the electron temperature for three different samples:  $d = 1400 \text{ \AA}$ , grating period  $a = 3 \text{ μm}$  (triangles);  $d = 1400 \text{ \AA}$ ,  $a = 1.5 \text{ μm}$  (squares);  $d = 6000 \text{ \AA}$ ,  $a = 3 \text{ μm}$  (inverted triangles). The antenna efficiency is normalized to  $\alpha = 0.025$ ; the integral is taken over the GaAs detector's linewidth of  $2.0 \text{ cm}^{-1}$ .

the intensities of subband emission from identical samples.<sup>11</sup> At temperatures above 13 K the plasmon emission intensity cannot be evaluated any more as a result of pinch-off effects in the inversion layer at high electric fields, which cause inhomogeneous electron heating.

Figure 3 (top) shows the normalized experimental emission intensity as a function of the electron density  $n_s$  at a constant frequency of  $\hbar\omega = 4.4 \text{ meV}$ . The maximum of the detector signal occurs for three different samples at different electron densities. The normalized total plasmon emission intensity decreases with increasing  $n_s$  according to Eqs. (3) and (4). In Fig. 3 (bottom) the normalized plasmon emission intensity is plotted versus the wave vector  $k$ . The dashed and full lines give the theoretical behavior for different oxide thicknesses and electron temperatures. The intensity increases with the square of the wave vector. This is confirmed accurately by the experimental data points obtained from four different samples.

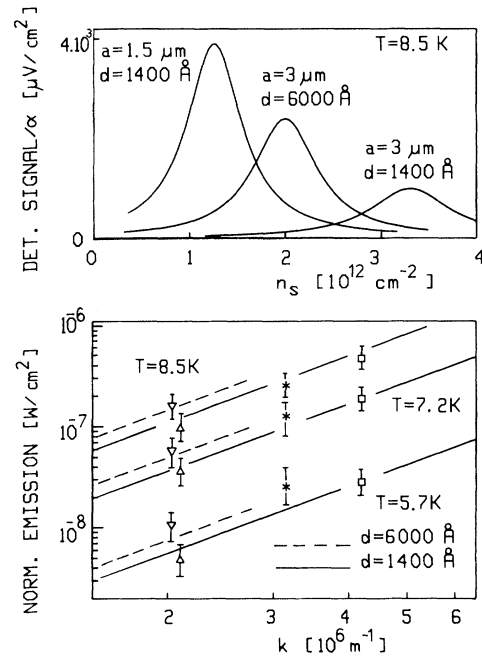


FIG. 3. Top: Experimental plasmon emission at constant  $\hbar\omega = 4.4 \text{ meV}$  as a function of the electron density. Bottom: Total intensity as a function of the plasmon wave vector for four different samples:  $d = 1400 \text{ \AA}$ ,  $a = 3 \text{ μm}$  (triangles);  $d = 1400 \text{ \AA}$ ,  $a = 1.5 \text{ μm}$  (squares);  $d = 6000 \text{ \AA}$ ,  $a = 3 \text{ μm}$  (inverted triangles);  $d = 2000 \text{ \AA}$ ,  $a = 2 \text{ μm}$  (asterisks). The theoretical emission intensities (curves) are plotted in the bottom figure according to Eq. (4);  $\alpha$  is normalized to  $\alpha = 0.025$ , and the integral is taken over  $2 \text{ cm}^{-1}$ .

In contrast to Ref. 7 it is found that samples with different orientation of the grating—parallel, tilted, and perpendicular to the current direction in the MOSFET—show the same intensity of far-infrared emission from 2D plasmon decay. This discrepancy can only be explained by a poor quality of the gratings with the wave vector perpendicular to the current. The present experiments were performed with high-quality gratings on the same sort of samples. This result excludes the possibility of the drift of the electron gas along the grating playing a role for the excitation, as would be the case in free-electron effects (Smith-Purcell effect, traveling-wave tubes, etc.).

With the known energy density [Eq. (1)] one can also calculate the specific heat of the 2D plasmons: For a pure two-dimensional plasma dispersion— $\omega^2$  proportional to  $k$ —we obtain for the molar plasmon specific heat

$$C_{v, pl} = \frac{dU}{dT} \frac{N_A}{n_s} = N_A k_B \left( \frac{T}{T_0} \right)^4 \int_0^{x_{crit}} \frac{x^5 e^x dx}{(e^x - 1)^2}, \quad (6)$$

where

$$T_0 = \frac{\hbar e}{k_B} \left( \frac{n_s^{3\pi}}{m^{*2} \epsilon_0^2 (\epsilon_s + \epsilon_i)^2} \right)^{1/4}$$

and  $x_{crit} = \hbar \omega_{crit} / k_B T$ .  $N_A$  denotes the Avogadro number and  $\omega_{crit}$  the critical frequency (cutoff frequency), where the dispersion relation of the plasmon crosses the single-particle excitation regime.<sup>12</sup> There the plasmon does not exist any more as a well-defined mode. The temperature  $T_0$  is characteristic for the low-temperature plasmon specific heat. Typical values of  $T_0$  for Si are, e.g., 328 K for  $n_s = 1 \times 10^{12} \text{ cm}^{-2}$  and 35 K for  $n_s = 0.5 \times 10^{11} \text{ cm}^{-2}$ . At low temperatures and high densities  $x_{crit}$  can be replaced by  $\infty$ . In this regime the plasmon specific heat increases with  $T^4$  and decreasing  $n_s$ . At high temperatures and low densities the plasmon specific heat would be of the order of the free-electron specific heat, which is limited by  $N_A k_B$ . However, the plasmon and single-particle contributions to the total specific heat cannot be simply added, since the kinetic energy of electrons as single particles and their collective motion cannot be considered completely independent. In addition the upper limit  $x_{crit}$  becomes finite and limits the value of  $C_{v, pl}$ . Therefore Eq. (6) describes the plasmon contribution to the total specific heat of the system only at low temperatures and high densities. We expect, however, the total specific heat of the electron system to exceed the free-electron-gas

value as a result of plasmon generation at low densities and high temperatures, since the *restoring* forces in the plasma oscillations increase the time-averaged energy of the system.

In conclusion, we have shown that plasmon excitation in two-dimensional systems is possible as a thermal process by heating the electron gas. Especially at low group velocities (low densities, high wave numbers) the excitation becomes very effective. The radiative decay time via the grating is very short, and therefore this radiation process seems superior to spontaneous radiation processes in solids with radiative decay times on the order of  $10^{-4}$  to  $10^{-6}$  s in the millimeter and submillimeter ranges.<sup>13</sup> For spontaneous processes such as Landau emission<sup>14</sup> the dominating recombination processes (phonon emission) are non-radiative with lifetimes on the order of  $10^{-9}$  s. The radiative decay time of the plasmon, however, is in the present case only about 1 order of magnitude longer than the nonradiative lifetime. This makes this process much more effective. We therefore propose the thermal excitation of two-dimensional plasmons as a potential new candidate for application as narrow-band radiation sources in the FIR and infrared ranges.

This work was partly supported by the Fonds zur Förderung der Wissenschaftlichen Forschung, Austria (Project No. S 22/05) and by the European Research Office, London. We are grateful to Günther Stangl from the International Atomic Energy Agency, Vienna, for the photolithographic production of the gratings. The MOS samples were provided by Bell Laboratories, Murray Hill, N. J., and by the Naval Research Laboratories, Washington, D. C.

<sup>1</sup>For a review, see H. Raether, *Excitation of Plasmons and Interband Transitions by Electrons*, Springer Tracts in Modern Physics Vol. 88 (Springer, Berlin, 1980), p. 118.

<sup>2</sup>S. J. Allen, D. C. Tsui, and R. A. Logan, *Phys. Rev. Lett.* **38**, 980 (1977).

<sup>3</sup>T. N. Theis, J. P. Kotthaus, and P. J. Stiles, *Solid State Commun.* **26**, 603 (1978).

<sup>4</sup>T. Ando, A. B. Fowler, and F. Stern, *Rev. Mod. Phys.* **54**, 437 (1982).

<sup>5</sup>F. Stern, *Phys. Rev. Lett.* **18**, 546 (1967).

<sup>6</sup>T. N. Theis, J. P. Kotthaus, and P. J. Stiles, *Surf. Sci.* **73**, 434 (1978).

<sup>7</sup>D. C. Tsui, E. Gornik, and R. A. Logan, *Solid State Commun.* **35**, 875 (1980).

<sup>8</sup>D. J. Olego, A. Pinczuk, A. C. Gossard, and

W. Wiegmann, Phys. Rev. B **25**, 7867 (1982).

<sup>9</sup>N. W. Ashcroft and N. D. Mermin, *Solid State Physics* (Holt, Rinehart and Winston, New York, 1976), Chap. 23.

<sup>10</sup>D. Pines, *Elementary Excitations in Solids* (Benjamin, New York, 1977).

<sup>11</sup>E. Gornik and D. C. Tsui, Solid State Electron. **21**,

139 (1977).

<sup>12</sup>P. M. Platzmann and P. A. Wolff, *Waves and Interactions in Solid State Plasmas* (Academic, New York, 1973).

<sup>13</sup>W. Müller, F. Kohl, H. Partl, and E. Gornik, Solid State Electron. **21**, 235 (1978).

<sup>14</sup>E. Gornik, Phys. Rev. Lett. **29**, 575 (1972).

## Observation of Heavy-Ion-Induced Wake-Potential Interference Effects

H. J. Frischkorn, K. O. Groeneveld, P. Koschar, R. Latz, and J. Schader

*Institut für Kernphysik der J. W. Goethe-Universität, D-6000 Frankfurt am Main, Germany*

(Received 27 September 1982)

The superposition of the wake potentials of Coulomb-exploding fragments of diatomic molecular projectiles penetrating a solid cause potential oscillations at the surface. The total electron yield per projectile serves as a signal to detect these oscillations. The plasma frequency of the solid and the wake-potential wavelength can be deduced from the data.

PACS numbers: 79.20.Rf, 34.90.+q

Energetic ions penetrating solids induce a cylindrically symmetric wake of electron-density fluctuations behind the projectile.<sup>1</sup> The damped periodic potential  $\Phi$  corresponding to these charge-density fluctuations is characterized by the charge  $Z_p$  and the velocity  $v_p$  of the projectile and by the dielectric function  $\epsilon(\omega_p)$  with the plasma frequency  $\omega_p$  of the solid.<sup>2,3</sup> Its wavelength  $\lambda_w$  is given by  $\lambda_w = 2\pi v_p / \omega_p$ . The influence of the charge-density fluctuations and their potential  $\Phi(Z_p, v_p, \epsilon)$  on the spectra of secondary electrons has been discussed previously<sup>4-6</sup> and the electron ejection of the solid has been predicted.<sup>4,6</sup>

These calculations prompted our previous experiments<sup>7</sup> where we studied the angular and energy distributions of low-energy ( $E_e < 50$  eV) electrons emitted from solids under energetic heavy-ion impact. The observed irregularities in the electron energy and angular distributions coincided with structures predicted by theory.<sup>4,6</sup> However, these results were inconclusive because of large experimental uncertainties.

In a novel approach to find the influence of the wake potential  $\Phi$  on electron emission from solids we measured the total (i.e., integrated over all emission angles and energies) electron emission per projectile ( $\gamma$ ) from solids (carbon). At equal velocities (isotachic) we compare the yields produced by monoionic projectiles  $C^+$  and  $O^+$  [ $\gamma(C)$  and  $\gamma(O)$ ] with the yield produced by the molecular projectile  $CO^+$  [ $\gamma(CO)$ ] and calculate the ratio

$R = \gamma(CO) / [\gamma(C) + \gamma(O)]$ . The ratio  $R$  is measured as a function of a quantity  $r_x / \lambda_w$  (see below) which is roughly proportional to  $t^2$  where  $t$  is the dwell time  $t = x / v_p$  of the projectile in the target with thickness  $x$ . A molecular-ion effect is observed if  $R(r_x / \lambda_w) \neq 1$ . Since most phenomena associated with  $v_p$  are monotonic functions of  $v_p$  in the velocity range of interest here we can vary either  $x$  or  $v_p$ .

The experimental setup is shown in Fig. 1. The basic idea is fairly simple, and the equipment inexpensive and quite appropriate to the present poor state of the world economy: Projectiles  $C^+$ ,  $O^+$ , and  $CO^+$  with  $1.5 \times 10^{10} \leq v_p \leq 4 \times 10^{10}$  cm/s are produced in a 2.5-MV Van de Graaff acceler-

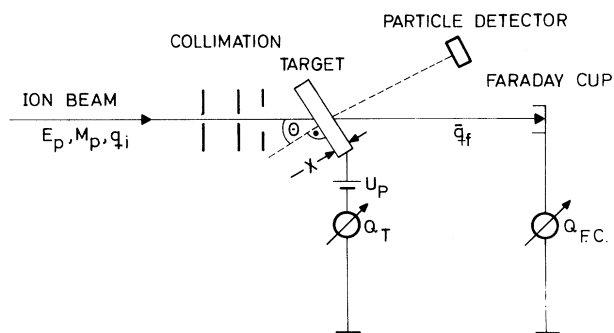


FIG. 1. Schematic presentation of the experimental setup. The symbols are explained in the text. In the present experiment the angle  $\theta = 0^\circ$ .